Sedimentation and Lithofacies Paleogeography in Southwestern China Before and After the Emeishan Flood Volcanism: New Insights into Surface Response to Mantle Plume Activity

Bin He,[1] *Yi-Gang Xu,*[2] *Ya-Mei Wang,*[1] *and Zhen-Yu Luo*

Key Laboratory of Geochronology and Geochemistry, Guangzhou Institute of Geochemistry, Chinese Academy of Science, Guangzhou, China 510640

ABSTRACT

Investigations into Permian sedimentation and reconstruction of paleogeography in SW China are aimed at characterizing sedimentary responses to the Emeishan mantle plume. In addition to erosional features on the sediments underlying the uplifted Emeishan basalts, unusual depositions of Permian age are also present in the Emeishan large igneous province (LIP). Specifically, carbonate gravity flows and submarine incised canyon fillings were developed in the western margin of the postulated uplifted area, and rifting trenches were developed along the eastern margin; alluvial fan deposits occur at the boundary between the inner and intermediate zones. These depositions all rest on the Maokou Formation and are in turn covered by the Emeishan basalts, implying synchronism between crustal uplift and depositional events. These deposits and the associated extension and normal faulting along the margin of and within the LIP represent sedimentary features resulting from dynamic behavior of mantle plume. Comparison of lithofacies paleogeography before and after the Emeishan flood volcanism highlights the determinant role of mantle plume activity in the geological evolution in SW China. The rapid, differential erosion of the Maokou Formation was likely related to plume-induced dynamic uplift. This uplift was apparently followed by subsidence, given deposition of the marine clastic rocks sandwiched between basalts and the Maokou Formation in the east and submarine basalts along the margins of the province. A second-phase uplift, attributed to underplating of plume-derived melts at the crust-mantle boundary, was characterized by prolonged (~45 m.yr.), plateau-type uplift and was responsible for the appearance of the "Chuandian old land." Integration of these erosional and depositional characteristics allows us to depict how the surface geology responds to mantle plume, which explains some complex sedimentological problems in SW China.

Introduction

The Permian sedimentation in SW China is one of the best exposed and studied in the world (Yang 1986; Jin et al. 1994). It has been widely known for a long time that the sedimentation in SW China before the Emeishan flood volcanism was characterized by a carbonate platform setting (Wang et al. 1994; Feng et al. 1997). However, a number of unusual depositions also occurred in this region during the Middle-Late Permian boundary, such as carbonate gravity flows, submarine incised canyon fillings, rifting trenches, and alluvial fan deposits. The dynamic mechanism and driving forces that led to the rapid transformation from a stable carbonate platform facies to "catastrophic" depositions before the Emeishan volcanism remain a puzzle. For instance, carbonate gravity flows in the western Emeishan large igneous province (LIP) were attributed to the formation of the slope system after the breakup of the carbonate platform in a passive continental margin during the genesis of a new ocean (Chen 1985; Zhang et al. 1988). However, it is unclear why deposits of a similar nature also occur in the interior of the craton. Moreover, the opening of the Songpan-Ganze ocean took place in the Late Permian and Triassic (Huang et al. 1992) and significantly postdated the formation of these catastrophic deposits. It seems that currently available individual models may apply in a given case, but they are not compatible with each other on a regional scale.

Manuscript received February 8, 2005; accepted August 23, 2005.

[1] China University of Geosciences, Wuhan, China 430074.

[2] Corresponding author; e-mail: yigangxu@gig.ac.cn.

[The Journal of Geology, 2006, volume 114, p. 117–132] © 2006 by The University of Chicago. All rights reserved. 0022-1376/2006/11401-0007$15.00

This content downloaded from 23.235.32.0 on Sun, 11 Oct 2015 09:15:18 AM
All use subject to JSTOR Terms and Conditions

It has recently been revealed that the Maokou Formation that lies immediately beneath the Emeishan basalts was systematically thinned, suggesting rapid, kilometer-scale prevolcanic crustal doming (He et al. 2003). Consistent with the prediction by theoretical modeling (Campbell and Griffiths 1990; Farnetani and Richards 1994), this has been taken as supporting evidence for the involvement of a mantle plume in the generation of the Emeishan flood volcanism (He et al. 2003; Xu et al. 2004). It is noted that the above-mentioned unusual depositions all rest on the Maokou Formation and are in turn covered by the Emeishan basalts, implying synchronism between crustal uplift and depositional events. It is thus pivotal to investigate whether these spatially scattered, diverse sedimentary features can be reconciled with a mantle plume model.

This article extends our sedimentological study of the Emeishan LIP (He et al. 2003) by describing and discussing the synuplift catastrophic depositions along the margins of the Emeishan LIP and comparing the sedimentation and paleogeography in SW China before and after the eruption of the Emeishan flood basalts. It will be shown that changes in sedimentation, tectonic evolution, and massive igneous activity during the Permian and Triassic in SW China can be nicely accommodated in a plume-based model. The results significantly complement our current understanding of the surface response to mantle plumes.

Geological Background and Previous Studies

The Late Permian Emeishan basalts are erosional remnants of the voluminous mafic volcanic successions occurring in the western margin of the Yangtze Craton, SW China. They are exposed in a rhombic area of 250,000 km^2 (Xu et al. 2001) bounded by the Longmenshan thrust fault in the northwest and the Ailaoshan–Red River slip fault in the southwest (fig. 1). However, some basalts and mafic complexes exposed in the Simao basin, northern Vietnam (west of the Ailaoshan fault), and in the Qiangtang terrain, the Lingjiang-Yanyuan belt, and the Songpan active fold belt (northwest of the Longmenshan fault) make possible an extension of the Emeishan LIP (Chung et al. 1998; Xiao et al. 2003; Hanski et al. 2004). The Emeishan flood volcanism succession comprises predominantly basaltic flows and pyroclastic deposits, with minor amounts of picrites and basaltic andesites, with a total thickness ranging from several hundred meters to 5 km (Xu et al. 2001). The Emeishan flood basalts have been divided into two major magma types: high-Ti ($Ti/Y > 500$) and low-Ti ($Ti/Y < 500$) basalts (Xu et al. 2001). In general, the high-Ti basalts have relatively higher $\varepsilon_{Nd}(t)$ and lower $^{87}Sr/^{86}Sr(t)$ values than the low-Ti basalts. Available data reveal a systematic spatial variation in basalt type. Specifically, the western Emeishan LIP comprises thick (2000–5000 m) sequences of dominant low-Ti volcanic rocks and subordinate picrites (Chung and Jahn 1995; Zhang and Wang 2002) and high-Ti and alkaline lavas (Xu et al. 2001, 2003; Xiao et al. 2003). In contrast, thin sequences (<500 m) of high-Ti volcanic rocks occur mainly in the eastern Emeishan LIP. It has been shown that the high- and low-Ti lavas require very different mantle conditions (Xu et al. 2001). Thus, this spatial variation reflects the thermal gradient of the mantle from which the Emeishan basalts were derived (Xu et al. 2004).

The Emeishan volcanic successions unconformably overlie the late Middle Permian carbonate (i.e., the Maokou Formation) and are in turn covered by the uppermost Permian sedimentary rocks in the east and Late Triassic sedimentary rocks in the central part of the Emeishan LIP. Figure 2 summarizes the regional variation of the Permian and Triassic stratigraphic sequences in the Emeishan LIP and its neighboring area. The Permian strata below the Emeishan basalts can be divided, in ascending order, into the Liangshan Formation (lower Permian) and the Qixia and Maokou formations (Middle Permian). The Middle and upper Permian strata in the upper Yangtze Craton are separated by an unconformity referred to as the Dongwu unconformity (ECS 2000). In most cases, the Emeishan basalts directly cover the Maokou Formation. The exception is noted in the marginal zone of the Emeishan LIP (*A*–*B* and *I* in fig. 1), where the Pingchuan and Baxian formations were developed between the Emeishan basalts and the Maokou Formation (fig. 2). These unusual sedimentary sequences are suggestive of local crustal deformation/faulting. The upper Permian sequences are variable along the west-east profile of the Emeishan LIP (fig. 2). In particular, the upper Permian is absent in the center of the Emeishan LIP (fig. 2). The upper Permian sequences include the Xuanwei Formation, composed of terrestrial clastic rocks, and the Longtan Formation, composed of marine clastic rocks. The standard upper Permian strata in South China are the Wujiaping and Changxing formations, which are composed mainly of limestones and biograin limestones. These formations are present in the eastern part (outer zone) of the Emeishan LIP (figs. 1, 2).

To characterize the area before the Emeishan volcanism, He et al. (2003) correlated and compared the biostratigraphic units of the Maokou Formation

This content downloaded from 23.235.32.0 on Sun, 11 Oct 2015 09:15:18 AM
All use subject to JSTOR Terms and Conditions

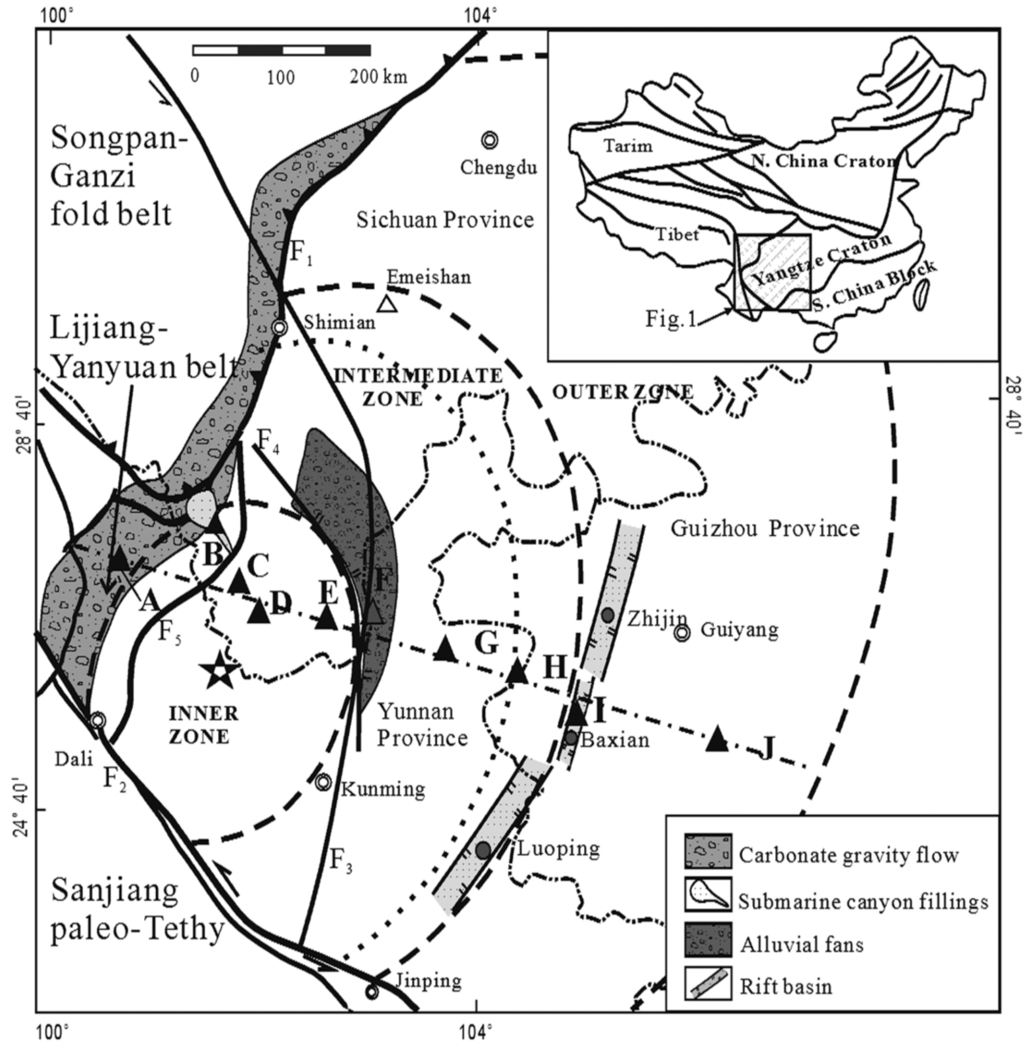

Figure 1. Map showing geology of the Emeishan large igneous province (LIP) and distribution of prevolcanic catastrophic depositions. Dashed lines separate the inner, intermediate, and the outer zones, which are defined in terms of erosion extent of the Maokou Formation (He et al. 2003). The dotted line outlines a region in the east of the LIP where subsidence-related deposition took place after domal dynamic uplift and before the eruption of Emeishan basalts. The dash-dotted line indicates the profile of the Permian and Triassic stratigraphy across the Emeishan LIP shown in figure 3. Solid lines labeled "F" indicate faults: F_1 = Longmenshan thrust fault; F_2 = Ailaoshan–Red River fault; F_3 = Xiaojiang fault; F_4 = Xichang-Qiaojia fault; F_5 = Jinhe fault. Note that the dimension of the Emeishan LIP is roughly in accordance with the dimensions of the inner and intermediate zones.

and showed a systematic thinning of the strata beneath the Emeishan basalt. The surface of thinned carbonates is an unconformity with karst paleotopography and local basal conglomerates, the clasts of which were derived from the uppermost Maokou Formation. This suggests that stratigraphic thinning likely resulted from differential erosion due to regional uplift. Isopachs of the Maokou Formation further delineate a circular uplifted area (He et al. 2003) very similar to the crustal doming above an upwelling mantle plume predicted by theoretical modeling (Campbell and Griffiths 1990). The domal structure associated with the Emeishan LIP is 800 km in radius and can be divided into inner, intermediate, and outer zones (fig. 1) in terms of the extent of erosion of the Maokou Formation. The duration of the uplift is estimated to be less than 3 m.yr., and the magnitude of uplift is greater than 1000 m (He et al. 2003). There is no known process on Earth, other than mantle plumes, that can form lithospheric domes 1000 km or more in radius and >1 km high within 3 m.yr.

This content downloaded from 23.235.32.0 on Sun, 11 Oct 2015 09:15:18 AM
All use subject to JSTOR Terms and Conditions

Stratum		Area: A-B	C-E	F-H	I	J
Triassic	Upper	T_3	T_3	T_3	T_3	T_3
	Middle	T_2	Chuandian old land	T_2	T_2	T_2
	Lower	Feixianguan		Feixianguan	Feixianguan	Yeliang
Permian	Upper	"Longtan"		Xuanwei Longtan	Changxin Linghao	Changxin Wujiaping
		Emeishan basalts	Emeishan basalts	Emeishan basalts	Emeishan basalts	
	Middle	Pingchuan			Baxian	Maokou
		Maokou	Maokou	Maokou	Maokou	
		Qixia	Qixia	Qixia	Qixia	Qixia
	Lower	Liangshan	Liangshan	Liangshan	Liangshan	Liangshan

Figure 2. Permian and Triassic stratigraphic correlation in the Emeishan large igneous province and its adjacent area. The locations of areas *A–J* are marked in figure 1. Dashed lines represent unconformities.

Preuplift Sedimentation and Lithofacies

The Maoukou Formation, immediately under the Emeishan basalts, has been extensively studied in China because of its widespread distribution and extremely abundant fossils (Wang et al. 1994; Feng et al. 1997; ECS 2000). It consists mainly of medium bedded to massive biograin limestones and biograin micritic limestones, with its original thickness ranging from 250 to 500 m (fig. 3). On the basis of rock types and textures, as well as fossil variety (e.g., foraminifera, algae, brachiopods, and ostracods), it is inferred that the water depth was possibly less than 20–50 m and that the depositional environment was a carbonate platform (i.e., corresponding to a stable tectonic setting). This carbonate platform, known as pan-Yangtze land (e.g., Chen 1985; Wang et al. 1994), covers an area much larger than the Emeishan LIP. Such a homogenous lithofacies is critical because it serves as a simple reference point from which any subsequent change can be measured. Because the subaerial Emeishan basalts directly overlie the paleokarst of the Maokou Formation, it can be suggested that crustal uplift and the emplacement of Emeishan basalts was a rapid event.

Synuplift Depositions before the Emeishan Volcanism

Carbonate Gravity Flow Sediments. In the central uplifted area, the Maokou Formation was eroded during the Late Permian. However, sedimentation continued in the western margin of the Emeishan LIP during the Permian, as shown by carbonate gravity flow sediments (Chen 1985; BGMRSP 1991; Liang et al. 1991, 1994) between the Maokou Formation and the Emeishan basalts (*A* in fig. 3). Carbonate gravity flows, with thickness varying from a few to 70 m, are distributed in a zone 80–300 km

Figure 3. Generalized stratigraphy of Permian and Triassic successions across the Emeishan large igneous province (LIP; the top of the Middle Triassic is assumed to be located at the same level). The location of each section is shown in figure 1. Prevolcanic catastrophic deposits are highlighted in some successions. The number near the stratigraphic unit indicates the thickness of the unit. The vertical scale is the same for each section. Data are compiled from Chen (1985), BGMRGP (1987), BGMRSP (1991), and He at al. (2003). P_2m^1 = *Neoschwagerina simplex* zone of Maokou Formation (Fm.); P_2m^2 = *Neoschwagerina craticulifera–Afghanella schencki* zone of Maokou Fm.; P_2m^3 = *Yabeina-Neomisellina* zone of Maokou Fm.; P_2pc = Pingchuan Fm.; P_2b = Baxian Fm.; P_3w = Wujiaping Fm.; P_3lh = Linghao Fm.; P_3e = Emeishan basalts; P_3ch = Changxing Fm.; P_3x = Xuanwei Fm.; P_3l = Longtan Fm.; T_1f = Feixianguan Fm.

This content downloaded from 23.235.32.0 on Sun, 11 Oct 2015 09:15:18 AM
All use subject to JSTOR Terms and Conditions

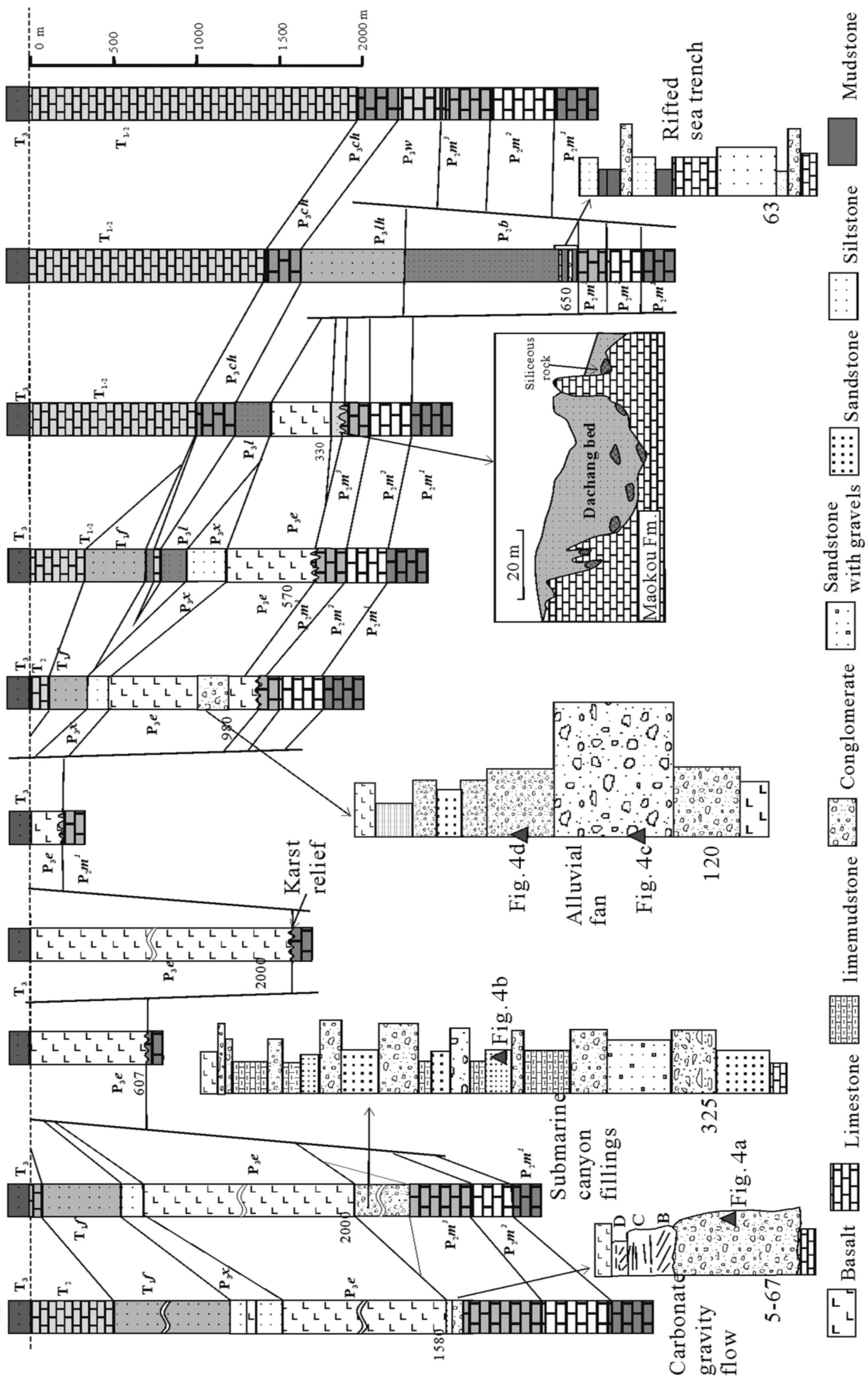

This content downloaded from 23.235.32.0 on Sun, 11 Oct 2015 09:15:18 AM
All use subject to JSTOR Terms and Conditions

wide and about 1000 km long (fig. 1) along the western flank of the domal structure.

Carbonate gravity flows consist of debris flows and subordinate turbidites (*A* in fig. 3). The debris flows contain various calcareous intraclasts and para-autochthonous fragments, which are poorly sorted and randomly distributed in a matrix of micrite. The intraclasts vary in size from several to 20 cm in diameter and are predominantly composed of biograin, arenaceous, and siliceous limestone, with subordinate amounts of carbonaceous slate, flints, and siliceous rocks. Some limestone intraclasts were crumpled irregularly, with one embedding into another, forming a jigsaw structure. Large intraclasts are mainly tabular, with an aspect ratio greater than 10. Two sorts can be distinguished. The first type is gray-white and light gray in color (fig. 4*a*). Fossils in these rocks, including foraminifera, algae, brachiopods, ostracods, corals, echinoderms, and gastropods, are typical of those occurring in a carbonate platform, indicating that these are not autochthonous and were likely derived by reworking the carbonate platform in shallow water. Another kind of debris is dark gray and gray-black micrite about 1–2 cm in diameter with subrounded and subangular shapes. The matrix of these rocks is composed of dark lime mud and minor sands, biograin, and clay. Calcareous turbidites overlie debris flow deposits in this zone and are composed mainly of calcareous sands and silts with a Bouma sequence of the B, C, and D divisions (*A* in fig. 3).

The occurrence of the carbonate gravity flows on the stable carbonate platform suggests a dramatic change in the sedimentary environment in the late Middle Permian. Development of these gravity flows requires lateral variation in morphology and conditions of sedimentation as well as the mechanism to induce gravity flow. Typically, gravity flow deposits are associated with a slope (Mullins and Neumann 1979). In the Emeishan case, roughly linear gravity flow deposits were distributed along the western flank of the inner zone (fig. 1). Slope and base-of-slope sedimentary systems are expected to develop in this transition zone, most likely as a consequence of synuplift normal faulting (Chen 1985; Zhang et al. 1988; Liang et al. 1994). With development of the domal uplift and rifting in the western margin of the LIP, materials derived from the uplifted region were transported and accumulated in a submarine slope and basin.

In summary, a major event must have occurred at the late Middle Permian, transforming the platform facies to a slope environment. The absence of gravity flows after the volcanism suggests that this platform-slope environment system was short-lived and disappeared suddenly when the massive flood basalt erupted on it.

Submarine Canyon Fillings. A 325-m-thick layer of marine conglomerate, sandstone, lime mud, and mudstone (i.e., the Pingchuan Formation; BGMRSP 1991) between the Maokou Formation and the Emeishan basalts at Pingchuan in the western margin of the province (*B* in figs. 1, 3) is preserved in a narrow zone less than 10 km wide. Conglomerate clast types include carbonate, quartz, and fossil clasts that resemble those in the Maokou and Qixia formations (fig. 4*b*). Conglomerates show the characteristics of debris flow deposits. Most sandstones are lithic in nature, but some are quartzose sandstones with foraminifera typical of the Maokou and Qixia formations (fig. 4*b*). These, together with the absence of feldspar and mica, suggest that these sandstones may have been derived from a weathered and erosional area of the Maokou and Qixia formations and the Early Permian Liangshan Formation, which mainly consists of quartzose sandstones. The Pingchuan Formation has at least three sedimentary cycles (micrite, sandstone, and conglomerate; fig. 4*b*). These rocks are massive, lack bedding, and are poorly sorted but display flute casts, grooves, and synsedimentary deformation structures.

As indicated above ("Preuplift Sedimentation and Lithofacies"), the preuplift Permian sedimentary environment was a stable carbonate platform. The sudden appearance of Pingchuan clastic rocks is therefore indicative of an abrupt change in style of sedimentation. It is also important to note that this is the only place in the western margin of Yangtze Craton where clastic rocks (mainly consisting of carbonate and quartzose sandstones) were developed below the Emeishan basalts (BGMRSP 1991). The composition and distribution of the Pingchuan Formation differ from those of the carbonate gravity flow deposits. Given that these clastic rocks are located between the uplifted region and the slope-basin environment in the western flank of the domal structure, we tentatively interpret them as fillings of submarine canyons, generated during the domal uplift. In this sense, the Pingchuan Formation is comparable to submarine canyons at modern continental margins, which act as conduits for debris and turbidity currents, particularly when sea level is relatively shallow. The Pingchuan Formation merges distally from the submarine slope system where debris flow deposits and turbidites are accumulated.

Extensional Rifting Sea Trench. Three rift basins, namely, the Luoping, the Baxian, and the Zhijin,

This content downloaded from 23.235.32.0 on Sun, 11 Oct 2015 09:15:18 AM
All use subject to JSTOR Terms and Conditions

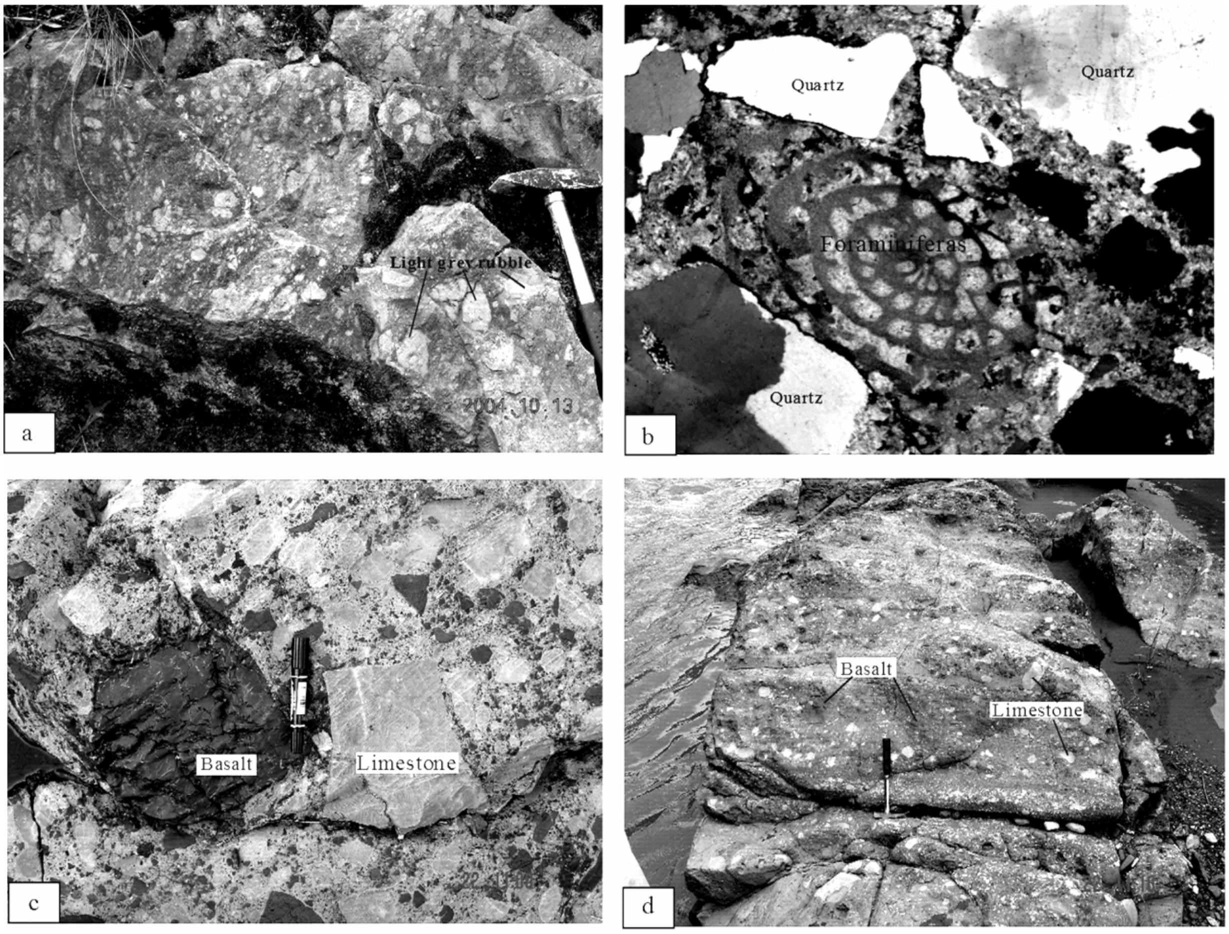

Figure 4. Photographs illustrating characteristics of prevolcanic depositions in the Emeishan large igneous province. *a*, Calcirudite contains two kinds of intraclasts: light gray and black-gray. *b*, Microphotograph showing quartz and biograin (fusulinid foraminiferas from Maokou Formation) cemented by calcium in quartzose sandstone. *c*, Subangular and angular limestone (*gray*) and basalt (*black*) conglomerates in alluvial fan deposits (section *F* in fig. 3). *d*, Graded bedding in the upper part of the alluvial fan deposits. The gravels of conglomerates are rounded and subrounded. Fine clastic rocks are carbonaceous sandstones.

were developed on the Maokou carbonate platform in the eastern Yunnan and western Guizhou provinces (fig. 1). They are interpreted as rifting at the late Maokou and/or early Wujiaping stage on the eastern margin of the Emeishan LIP, in contrast to the stable carbonate platform setting that prevailed during the Middle Permian in SW China (Feng et al. 1997).

The Baxian basin, 30 km wide and 200 km long, is located in Baxian County in western Guizhou (fig. 1; *I* in fig. 3). The sediments (i.e., the Baxian Formation) in this basin, with an average thickness of 650 m, conformably overlie the Maokou Formation. They include siltstones, claystones, and limestones. Limestones that are interbedded with the siltstones contain foraminifera such as *Neomisellina* sp., *Neoschwagerina* sp., *Codonofusiella* sp., *Reichelina* sp., and *Dunbarula* sp., typical of the top unit of the Maokou Formation. This suggests that the Baxian Formation is of Middle Permian age and predates the main eruption of the Emeishan basalts. On the basis of rock association and its spatial distribution, the Baxian Formation is interpreted as sediments of a deep-sea trench bounded by two normal faults (BGMRGP 1987). It is interesting that this deep-sea trench disappeared at the end of the Wujiaping stage and is therefore roughly coeval with the crustal uplift.

The Zhijin basin is interpreted as a late Middle Permian rift in central Guizhou Province (fig. 1; Luo et al. 1990; Zhao 1991). This NE-trending basin is 15–45 km wide and 140 km long. Unlike the

This content downloaded from 23.235.32.0 on Sun, 11 Oct 2015 09:15:18 AM
All use subject to JSTOR Terms and Conditions

clastic deposits in the Baxian basin, the Zhijin basin includes thin-bedded siliceous rock, siliceous shale, shale, pyroclastic rock, basalts, and minor ammonites, sponge, radiolaria, and siliceous sponge spicules. The fossil assemblage in this basin is typical of a deep-sea environment. This contrasts with the sedimentary rocks outside of the Zhijin basin, which are carbonates of a shallow-water platform (Luo et al. 1990; Zhao 1991). Such differential sedimentation over a restricted area lasted for only a very short period, because the development of the Zhijin basin on the carbonate platform started during the early Maokou stage and ended at the end of Maokou stage.

Like the Baxian basin, the Luoping basin in eastern Yunnan is defined mainly by the narrow distribution of thick marine clastic rocks of Late Permian age, i.e., the Longtan Formation. The average thickness of this basin is 700 m, which is significant in comparison with the 150–200-m thickness on the eastern margin of the Emeishan LIP (Wang et al. 1994; Feng et al. 1997). This depositional pattern is consistent with the fact that this basin was controlled by two boundary synsedimentary normal faults (BGMRGP 1987). Sediments of the Luoping basin are mainly fine clastic rocks, derived from a basaltic source.

Although different in detail, three basins share some similar features. (1) They were all formed on the carbonate platform at the late Maokou stage and shrank some time after the main eruption of the Emeishan basalts. (2) These narrow rift basins were all roughly NE-trending and controlled by normal faults. (3) They are all distributed in the eastern part of the Emeishan LIP, constituting parts of an undeveloped ring depression. (4) Most of the sedimentary rocks in these basins (especially in the Baxian and Luoping basins) were derived from the erosion and weathering of the Emeishan basalts. These characteristics lead us to propose that this depression may be related to thermal decay after the eruption of the basalts.

Alluvial Fan Deposits. A 65–172-m layer of coarse clastic rocks occurs within the lower part of the Emeishan basalt successions in the northeastern margin of the inner zone. They are distributed within an area 400 km long and 30–80 km wide along the Xichang-Qiaojia fault (F_4 in fig. 1). This clastic layer consists mainly of conglomerates (about 95% of the layer; *F* in fig. 3) that are very poorly sorted and contain boulders up to 1 m in diameter near the fault. The conglomerate is 50%–80% boulders and gravels that are mostly limestones of the Maokou Formation and subordinately basalt. In particular, the conglomerates near the Xichang-Qiaojia fault contain clasts that are exclusively limestones, 10–50 cm in diameter and angular, subangular, and subround in shape (fig. 4*c*). The matrix, consisting of angular to subrounded sand- and silt-sized carbonate rock fragments, is cemented by calcium and clay. The rocks in the upper part of the conglomerate layer have graded bedding (fig. 4*d*) in some places. Sandstones are subordinately developed above the conglomerate layer. It is interesting that the grains of sandstones are mainly limestones and biograins (60%–90%). These fine clastic rocks have abundant sedimentary structures, such as graded bedding and parallel bedding. Distribution and development of these coarse clastic rocks were apparently controlled by the Xichang-Qiaojia fault. The conglomerate layer is thickest (172 m) near the fault and becomes gradually thinner and finally disappears away from the fault. The content and size of gravels in the conglomerate layer also change regularly from west to east. Specifically, the conglomerates near the Xichang-Qiaojia fault are entirely composed of eroded materials from the uppermost Maokou Formation, whereas basalt clasts occur in the areas distal from the fault. Clast size decreases gradually from 10–50 cm (up to 1 m) to 3–5 cm from west to east in the profile. We thus propose that these coarse clastic rocks represent alluvial fan deposits that resulted from rapid crustal uplift and normal faulting between the inner and intermediate zones. The major component of Maokou limestones in alluvial conglomerates suggests that the Maokou Formation was subaerially exposed in the inner zone before massive flood volcanism.

Subsidence Deposits on the Paleokarst of the Maokou Formation. The Emeishan basalts were erupted subaerially on the karst of the Maokou Formation over most of the postulated area of uplift. However, a layer of marine sedimentary rocks (i.e., the "Dachang bed"; BGMRGP 1987) with variable thickness (0–85 m) was developed between the paleokarst of the Maokou Formation and the Emeishan flood basalts (fig. 1; sketch of *H* in fig. 3) along the eastern margin of the domal structure (i.e., the outer zone; fig. 1). Because the paleokarst of the Maokou Formation is considered to have been developed as a result of crustal uplift (He et al. 2003), it follows that the formation of the Dachang bed took place after the early crustal uplift but before the Emeishan volcanism. The Dachang bed is composed mainly of clastic rocks, with minor limestone and siliceous rock. Fossils in these deposits, such as *Neomisellina* sp. and *Neoschwagerina* sp., are typical of the upper Maokou Formation (He et al. 2003). The presence of limestone and siliceous

This content downloaded from 23.235.32.0 on Sun, 11 Oct 2015 09:15:18 AM
All use subject to JSTOR Terms and Conditions

rocks in the Dachang bed suggests that they were formed in a marine environment. This implies that subsidence must have occurred after the crustal uplift but before the volcanism in the outer zone of the Emeishan LIP. This subsidence is further supported by submarine eruption of basalts, as indicated by limestones that interbedded with the Emeishan basalts in this area (e.g., at Zhijin, Hongxian; Thomas et al. 1998). The isopachs of the Emeishan basalts (fig. 5*b*) indicate that submarine eruption of basalts was restricted to the outer zone, where the relative crustal uplift was minor. The lack of marine deposition in the inner and intermediate zones may be related to the fact that crustal uplift in these regions was larger than the magnitude of subsidence or that subsidence was compensated for by crustal uplift caused by magmatic underplating (see "Discussion").

Posteruptional Sedimentation and Lithofacies Paleogeography

Systematic stratigraphic study and paleogeographic reconstruction reveal a dramatic change in sedimentary environment before and after the Emeishan volcanism in SW China (fig. 5; Wang et al. 1994; Xu et al. 2004). The most striking change is the appearance of an elliptical basement core (known as the "Chuandian old land") in the center of the Emeishan LIP (fig. 5*c*). The Chuandian old land was likely exposed as a consequence of the domal uplift and accumulation of voluminous flood basalts. This old land was surrounded by terrigeneous (Xuanwei Formation) and marine (Longtan Formation) clastic rocks after the Emeishan volcanism (fig. 5*c*, 5*d*). Depositional patterns from the upper Permian to the Middle Triassic show transgression, as marine clastic rocks and limestones progressively overlapped the Chuandian old land (figs. 3, 5*c*–5*e*). However, it is interesting that a large regression occurred globally during the Late Permian (Wang et al. 1994). This implies that the relative sea level drop in the Middle-to-Late Permian of the Emeishan LIP was a local tectonic phenomenon.

The tectonic setting of this area was significantly affected by the closure of paleo-Tethys in the Late Triassic. The ubiquitous presence of upper Triassic sediments in SW China marked the disappearance of the Chuandian old land. The total thickness of the strata above the Maokou Formation and below the Late Triassic in the east of the Emeishan LIP is about 2000 m (figs. 3, 5*c*–5*e*). This means that the relief between the inner zone and the intermediate and outer zones was about 2000 m.

Discussion

Formation of Catastrophic Depositions before the Emeishan Volcanism. As stated in the "Introduction," the spatially scattered, diverse catastrophic sedimentary features described in this article and in the literature have puzzled geologists for a long time and cannot be reconciled with a simple tectonic model. It should be indicated that all catastrophic depositions are time constrained between the Maokou Formation and the Emeishan basalts (fig. 3). No such depositions occurred after the Emeishan volcanism. If the erosion of the Maokou Formation was related to crustal doming by a mantle plume (He et al. 2003), it can be inferred that the catastrophic deposition occurred simultaneously with or after the domal uplift but immediately before the eruption of Emeishan basalts and that the sedimentary sequences in the Late Permian changed dramatically over a rather short period. We propose that the initial stable carbonate platform setting during the early Middle Permian was broken up in the late Middle Permian by rapid crustal doming. The occurrence of platform-type carbonate in the outer zone during the Late Permian suggests that crustal unstability lasted for only a few million years before the volcanism. In this sense, the formation of the catastrophic deposition was temporally related to the plume activity that led to the crustal elevation and the eruption of Emeishan basalts.

If the distribution of catastrophic deposits is viewed in the context of the domal uplift (He et al. 2003), it becomes clear that most of these deposits are distributed around the margins of the LIP, near the boundary between the inner and intermediate zones. Specifically, the gravity flows are located at the western flank of domal structure, the alluvial fan at the northeast flank of the dome, and the rifted sea trenches at the eastern margin of the Emeishan LIP.

The temporal and spatial distribution of these catastrophic deposits is therefore attributable to the mantle plume activity that led to the eruption of the Emeishan basalts. Mantle plumes, arising from the Earth's deep interior, are expected to leave considerable effects on the surface geology, such as rapid uplift (Crough 1983; White et al. 1987; Cox 1989; Campbell and Griffiths 1990; Griffiths and Campbell 1990; Farnetani and Richards 1994), faulting (Griffiths and Campbell 1991; D'Acremont et al. 2003), and rapid change in sedimentation and lithofacies (Rainbird 1993; Nadin et al. 1997; Dam et al. 1998; Williams and Gostin 2000; Rainbird and Ernst 2001). These effects fall into two categories:

This content downloaded from 23.235.32.0 on Sun, 11 Oct 2015 09:15:18 AM
All use subject to JSTOR Terms and Conditions

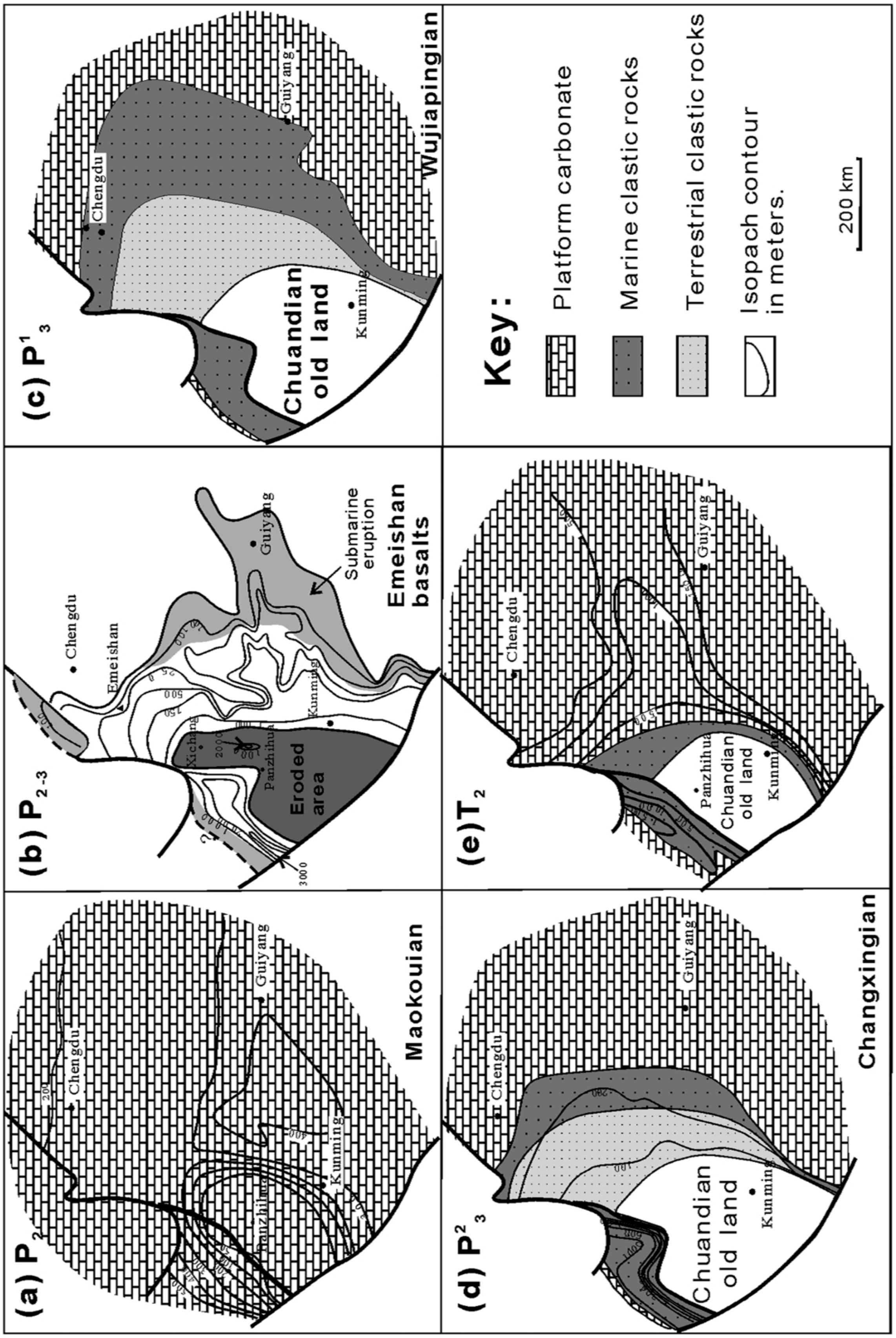

This content downloaded from 23.235.32.0 on Sun, 11 Oct 2015 09:15:18 AM
All use subject to JSTOR Terms and Conditions

erosional features (e.g., shoaling and thinning of strata, erosional unconformity, incised valleys, karst; Rainbird and Ernst 2001; He et al. 2003) and depositional responses (e.g., catastrophic deposition, rifting deposition, and an emergent trend in lithofacies; Rainbird 1993; Dam et al. 1998; Williams and Gostin 2000). Previous studies reveal that the Emeishan LIP provides perhaps the best example of erosional effects related to plume upwelling (He et al. 2003; Xu et al. 2004). It is argued here that it also documents the depositional response to a mantle plume.

The temporal and spatial distribution of these catastrophic deposits is consistent with the results of theoretical modeling concerning faulting and rifting during plume upwelling (Griffiths and Campbell 1991; D'Acremont et al. 2003). Griffiths and Campbell (1991) investigated the interaction of mantle plume heads with the Earth's surface by studying the behavior of a spherical blob of buoyant fluid and argued that there are at least three possible structures (i.e., arcuate trench, or graben, ring normal faults in the periphery of LIPs, and cell-like structures) associated with plume interaction with the crust. More recently, D'Acremont et al. (2003), using numerical modeling, suggested that plume head flattening could create a higher strain around the plume head, resulting in two areas of strong lithospheric thinning. These areas are associated with normal faulting and nucleate two rifting zones, each located at a horizontal distance of about 600 km from the plume head center (D'Acremont et al. 2003). The sequence and spatial distribution of the geological events in the Emeishan LIP are broadly similar to the results of this plume modeling. We thus interpret the alluvial fan as resulting from normal faulting during dynamic uplift and gravity flow deposits and the sea trenches as local extension/rifting resulting from stresses along the flattening of the plume head. An implication of this interpretation is that the Emeishan mantle plume head is ~1000 km in diameter, which is of the same order as the dimension of the Emeishan LIP. This estimate is significantly greater than that determined by the erosional records of Maokou Formation (about 400 km in diameter; He et al. 2003).

Similar plume-induced catastrophic depositions have been documented in other LIPs (White and Lovell 1997; Dam et al. 1998; Rainbird and Ernst 2001). In particular, Williams and Gostin (2000) described turbidites, gravity slides, and incised-canyon fillings in late Neoproterozoic successions in South Australia and interpreted them as a result of regional uplift, tectonic instability, and crustal extension caused by mantle plume activity. Clearly, these features share a number of similarities with those described in the Emeishan LIP. Nevertheless, it is necessary to indicate that the relationship between the catastrophic depositions and the structure of the corresponding mantle plumes is unclear in previous studies mainly because the latter is poorly defined. This renders it impossible to directly compare the catastrophic deposits with numerical modeling results. In this sense, the Emeishan LIP may be unique, and the documented features are useful to studies in other LIPs.

Comparison of Sedimentation Before and After Emeishan Volcanism: Evidence for Two Phases of Crustal Uplift. Figure 5 summarizes the paleogeographic evolution from the Middle Permian to the Triassic in the western Yangtze Craton. The Middle Permian was characterized by a vast carbonate platform. This platform was subjected to subaerial erosion to varying degrees in the late Middle Permian. The isopach for the remnant Maokou limestone is not randomly distributed but delineates a roughly subcircular shape (fig. 5*a*) that we interpret as the result of erosion of a domally uplifted terrain (He et al. 2003) due to plume impact on the base of the lithosphere. Plume uplift also influences the geography of the western Yangtze Craton until the Middle Triassic (fig. 5).

The distribution of the remnant Emeishan basalts appears to be dependent on this domal structure (fig. 5*b*). The absence of the Emeishan basalts in the uplifted area (i.e., the inner zone) must have been due to enhanced erosion of this uplifted area. The majority of the Emeishan basalts were sub-

Figure 5. Diagram showing changes in sedimentation and lithofacies paleogeography before and after the Emeishan volcanism. *a*, Stable, homogeneous carbonate platform in the Maokou stage (P_2) that is much bigger than the Emeishan large igneous province. The isopach contours of the remnant Maokou Formation indicate a domal thinning. *b*, Isopach contours of remnant Emeishan basalt (P_{2-3}). *c*, Paleogeography in the Wujiapingian (P_3^1). *d*, Lithofacies paleogeography in the Changxingian (P_3^2); the solid line indicates the isopach contours of the upper Permian strata. *e*, Lithofacies paleogeography in the Middle Triassic (T_2); the solid line indicates the isopach contours of lower and Middle Triassic strata. Data compiled from BGMRGP (1987), BGMRSP (1991), Wang et al. (1994), and Feng et al. (1997).

This content downloaded from 23.235.32.0 on Sun, 11 Oct 2015 09:15:18 AM
All use subject to JSTOR Terms and Conditions

aerially erupted; only small portions are submarine facies and are restricted to the margin of the Emeishan LIP (fig. 5*b*). This, together with the fact that the Dachang bed was deposited above the paleokarst of the Maokou Formation and was covered by the flood basalt in the eastern outer zone, strongly suggests a rapid subsidence after the uplift. These characteristics are predicted for dynamic-uplift processes in simulations (Griffiths and Campbell 1991).

The magnitude of dynamic uplift has been estimated from the erosional features of the overlying sedimentary sequence (He et al. 2003), assuming that the amount of dynamic uplift equates to that of erosion. However, this is complicated by the isostatic rebound effect. When the crust above the plume is eroded away, the crust rebounds, leading to more erosion, making it very difficult to estimate the amount of uplift.

The coincidence of the inner zone and the Chuandian old land (fig. 5*c*–5*e*) suggests that the latter resulted from plume-induced uplift. However, the dynamic uplift due to plume impact on the base of the lithosphere is basically transient and would vanish after a short time because of decay of the thermal anomaly and/or deflation of mantle head (Griffiths and Campbell 1990; Farnetani and Richards 1994; D'Acremont et al. 2003). This dynamic uplift, therefore, cannot explain the prolonged crustal uplift (~45 m.yr.) observed in the center of the Emeishan LIP, although thermal decay may be responsible for the retreat of the old land shown by progressive transgression (fig. 5*c*–5*e*). Such a prolonged uplift may be due to magmatic underplating (White et al. 1987; McKenzie 1984; Cox 1989; Brodie and White 1994), which in some instances may last for >200 m.yr. (Cox 1989). Another indication of the uplift due to magmatic underplating, which is superimposed on the early dynamic uplift, is provided by the uplift curve because the curve of the underplating uplift is homogenous and of the plateau type, whereas the dynamic uplift is of the sine wave type (Griffiths and Campbell 1990; Nadin et al. 1997). The gradual decrease in remnant Emeishan basalts from the inner zone to the margin of the Emeishan LIP (fig. 5*b*) is likely related to the thermal structure of the mantle plume (Xu et al. 2001, 2004). Preservation of this distribution pattern suggests that the Emeishan basalts may have escaped erosion or that there was less erosion in the intermediate and outer zones; otherwise, a reverse trend would be expected. Therefore, the erosion of the Emeishan basalts was largely restricted to the inner zone. All these data indicate plateau-type uplift. Further supporting evidence for magmatic underplating in the Emeishan LIP comes from recent seismic tomographic data, which reveal a thick (ca. 20 km), high-velocity lower crust (V_p = 7.1–7.8 km/s) in the western Yangtze Craton (Liu et al. 2001). We thus conclude that both plume-induced dynamic uplift and underplating-related uplift played roles in Permo-Triassic crustal elevation of the western Yangtze Craton.

The magnitude of underplating uplift can be roughly estimated from the sedimentary record of the Late Permian to the Middle Triassic. Figure 5*d* shows that a very narrow ring of clastic rocks and limestones surround the Chuandian old land, suggesting that basalts above sea level were almost entirely eroded in the inner zone. The thickness from the base of basalts to the Middle Triassic is about 2000 m in the intermediate and outer zones. The relief between the inner and intermediate-outer zones has to be of the same order of thickness in order for the inner zone to be in a state of erosion while the eroded materials accumulated in the intermediate-outer zones. In this sense, the magnitude of uplift due to underplating is about 2000 m. McKenzie (1984) and MacLennan and Lovell (2002) argued that surface uplift is one-tenth of the thickness of magmatic underplating layer. Crustal elevation of 2000 m therefore implies an underplating layer 20 km in depth. This estimate is roughly consistent with seismic data that reveal a high-velocity layer 20 km thick in the lower crust (Liu et al. 2001; Xu et al. 2004).

A Unified Model Explaining Surface Geological Evolution during the Emeishan Plume Activity. Previous knowledge of the surface response to mantle plumes is largely built on erosional features, changes in facies, and processes over the uplifted area caused by the rising plume because these are recorded in sedimentary rocks of all ages from widely disparate geographic locations (Rainbird and Ernst 2001). However, as pointed out in the "Introduction," the erosional record tells only a part of the story. The depositional characteristics described in this study significantly complement/broaden our current understanding of the surface response to mantle plumes. In this section, erosional and depositional data are integrated to help trace how the surface geology evolved together with the plume activity in the western Yangtze Craton (fig. 6).

During the early Middle Permian, the western Yangtze Craton was overlain by a vast carbonate platform, indicating a stable preuplift tectonic setting (fig. 6*a*). Toward the end of the Middle Permian, this area became tectonically unstable, and the carbonate platform was broken up as a result of a rapid, kilometer-scale crustal doming in the center

This content downloaded from 23.235.32.0 on Sun, 11 Oct 2015 09:15:18 AM
All use subject to JSTOR Terms and Conditions

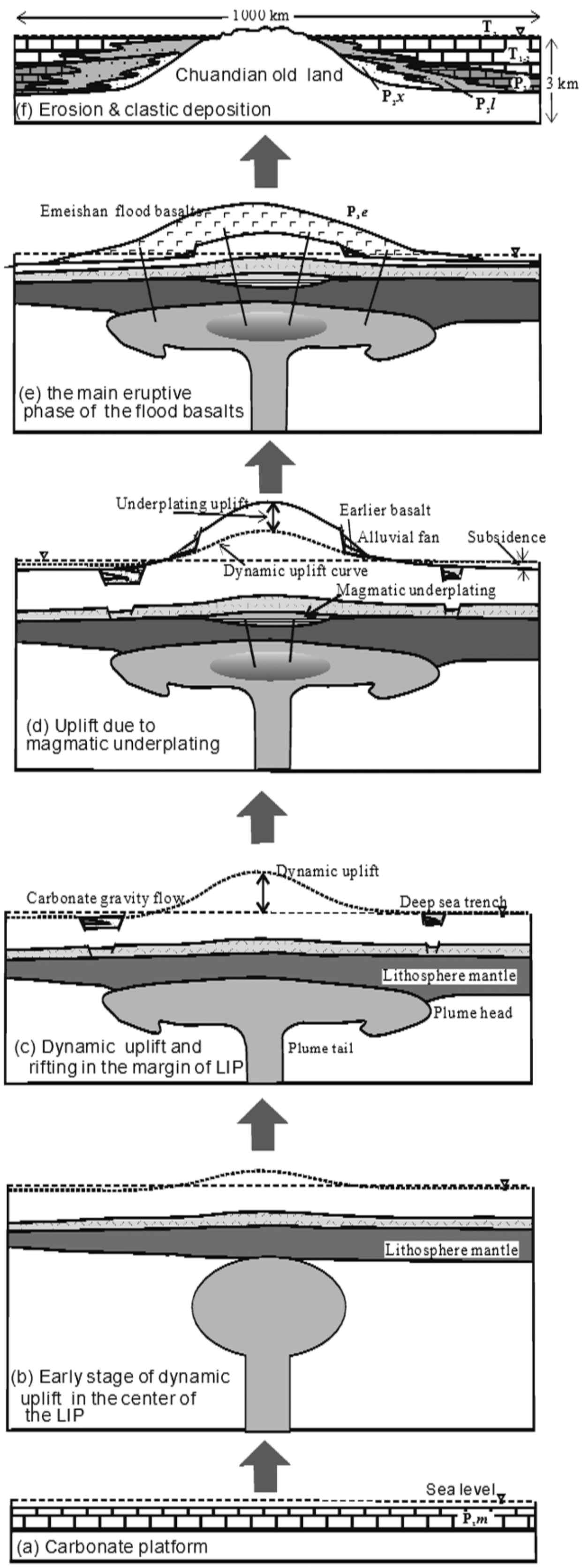

of the Emeishan LIP (He et al. 2003). The abrupt uplift of marine sediments above sea level allowed rapid differential erosion of the Maokou Formation. This erosion process not only resulted in beveling of the Maokou Formation but also created a paleokarst on top of it. The crustal uplift was dynamic in nature because of the impact of an ascending plume at the base of the lithosphere. The plume head at this stage was probably still spherical in shape (~400 km in diameter) and relatively deep, and so no significant melting occurred in the plume (fig. 6*b*). With its further ascent, the plume head started to collide with the base of lithosphere and spread out, forming a flattened head 800–1000 km in diameter (fig. 6*c*). At the same time, rifting and faulting (depression and extension) occurred around the margin of the Emeishan LIP, along with catastrophic depositions, such as gravity flow deposits (fig. 6*c*). It is interesting that rifting and depression were restricted to the plume periphery rather than the center of the LIP, which instead experienced uplift and erosion. Such features are predicted by

Figure 6. Cross section (or profile) cartoon through the Emeishan large igneous province (LIP) from west to east illustrating the surface responses to the Emeishan mantle plume (not to scale). *a*, Stable, homogeneous carbonate platform in the Middle Permian. *b*, The carbonate platform was broken up as a result of a starting mantle plume. The plume head at this stage was spherical in shape (~400 km in diameter) and relatively deep, and so no significant melting occurred. As a consequence, domal uplift (above sea level) took place only in the center of the LIP. *c*, With its further ascent, the plume head started to collide with the base of lithosphere and spread out, forming a flattened head 800–1000 km in diameter. At the same time, rifting and faulting (depression/extension) occurred around the margin of the LIP, most likely above the extremity of flattened plume head. This resulted in syndoming catastrophic depositions, such as gravity flow deposits. *d*, The plume started to produce high-magnesian melts that were trapped at the crust-mantle boundary. This magmatic underplating induced a second phase of crustal uplift, which exposed the Chuandian old land. *e*, Main eruptive phase of the Emeishan flood basalts. The duration is short; the thickness of the flood basalts decreases from the inner zone to the outer zone. *f*, Crustal elevation prevailed until the Late Triassic, the Chuandian old land was eroded continually, and weathering clasts were deposited in the intermediate-outer zones. It must be indicated that the scenarios depicted in *b*–*f* happened over a rather short period. Some processes are not mutually exclusive in terms of time and may have taken place simultaneously.

This content downloaded from 23.235.32.0 on Sun, 11 Oct 2015 09:15:18 AM
All use subject to JSTOR Terms and Conditions

theoretical modeling (Griffiths and Campbell 1990; D'Acremont et al. 2003)

A phase of rapid subsidence took place after paleokarst formation of the Maokou Formation. Alluvial fan deposits were developed within the lower part of the Emeishan basalt in the margin of the inner zone. Meanwhile, the mantle plume began to melt, producing high-magnesian melts, such as picrites (Chung and Jahn 1995; Zhang and Wang 2002). Because of their high density, these high-magnesian melts were largely trapped at different crustal levels (fig. 6*d*; Xu et al. 2004). While it remains uncertain whether the seismically imaged, high-velocity layer (>25 km) at the crust-mantle boundary (Liu et al. 2001) represents entirely underplated materials, it is possible that the emplacement of a huge volume of high-temperature ultramafic to mafic materials at the base of the crust induced a second phase of crustal uplift. Specifically, this uplift was responsible for the prolonged uplift (i.e., the Chuandian old land) before the Triassic.

These catastrophic deposition events were immediately followed by an outpouring of massive basalts that directly covered the uplifted region (fig. 6*e*). The residual crustal uplift promoted significant erosion of the Emeishan basalts in the inner zone such that there is greater preserved thickness of basalt in the intermediate and outer zones (fig. 5*b*). Comparison of paleogeographic patterns before and after the Emeishan volcanism (fig. 5) highlights the role of the Emeishan plume in surface geologic evolution in the western Yangtze Craton. It is noted that the isopachs of the Maokou Formation delineate a subcircular region that outlines the paleogeographic pattern during the upper Permian to Middle Triassic. It is from these observations that we conclude that the mantle plume that generated the Emeishan basalts caused the uplift that exposed the Chuandian old land and prevailed until the Triassic (fig. 6*f*). The Chuandian old land became progressively smaller from the upper Permian to the Middle Triassic, with increasing marine transgression in the western Yangtze Craton. This may be related in part to decay of the thermal anomaly generated by the proposed mafic underplating.

Conclusions

The Emeishan LIP is an excellent region in which to investigate the sedimentary response to a mafic magmatic event that is interpreted to have been generated by a mantle plume. In addition to erosional features that are widely recorded in many LIPs of different ages, the Emeishan LIP also preserves depositional features that are consistent with domal uplift related to plume activity. The main sedimentary characteristics related to the Emeishan mantle plume activity can be summarized as follows:

1. A rapid, kilometer-scale crustal doming in the core of the Emeishan LIP resulted in intensive erosion of the sedimentary sequence under the flood basalts over the uplifted area. In contrast, syndoming catastrophic deposition took place mainly in the margin of the LIP.

2. Catastrophic depositions include carbonate gravity flows, submarine canyon deposits, and alluvial fan deposits. They are related both in time and in space to the plume that we consider to be responsible for the generation of the Emeishan basalts. The first two deposits are distributed around the margin of the Emeishan LIP and may be related to depression/rifting above the periphery of the flattened plume head. The dimensions of the inner zone mirror those of spheric plume head, approximately 400 km in diameter, and the location of the intermediate zone defines the size of the flattened plume head, ~1000 km in diameter. The alluvial fan deposits resulted from topography generated by normal faulting between the inner and intermediate zones. These events are also temporally and spatially related to the crustal deformations induced by the impact of the Emeishan plume and are in good accord with modeling by Griffiths and Campbell (1991) and D'Acremont et al. (2003). These pre- and posteruption features are also similar to those outlined by Rainbird and Ernst (2001).

3. Two phases of crustal uplift have been identified, with the first, transient phase related to the dynamic impact of the plume head at the base of the lithosphere and the second, prolonged phase to magmatic underplating at the crust-mantle boundary.

4. Comparison of paleogeographic environment and sedimentation before and after the Emeishan volcanism highlights the determinative role of the Emeishan plume in the Permian to Triassic geological evolution in the western Yangtze Craton. A mantle plume may have been the ultimate driving force that caused (1) epeirogenesis (uplift, i.e., the Dongwu movement), rifting, and faulting between the Middle and Late Permian periods; (2) the transformation from stable carbonate platform deposition to catastrophic depositions that occurs between the Maokou Formation and the Emeishan basalt; and (3) the exposure of the Chuandian old land. In other words, the plume model provides an appropriate framework for understanding apparently unrelated, spatially scattered catastrophic depositions of the Late Permian in the western Yang-

This content downloaded from 23.235.32.0 on Sun, 11 Oct 2015 09:15:18 AM
All use subject to JSTOR Terms and Conditions

tze Craton, which have puzzled Chinese geologists for a long time.

ACKNOWLEDGMENTS

R. Rainbird and two anonymous reviewers are thanked for their careful and constructive reviews, which substantially improved the article. We gratefully acknowledge financial support from the National Natural Science Foundation of China (grants 40234046 and 40421303), the Chinese Academy of Sciences (the Bairen Project, grant KZCX2-101), and the Guangzhou Institute of Geochemistry (grant GIG-CX-04-06).

REFERENCES CITED

BGMRGP (Bureau of Geology and Mineral Resources of Guizhou Province). 1987. Regional geology of Guizhou Province. Beijing, Geological Publishing House, 698 p. (in Chinese with English abstract).

BGMRSP (Bureau of Geology and Mineral Resources of Sichuan Province). 1991. Regional geology of Sichuan Province. Beijing, Geological Publishing House, 745 p. (in Chinese with English abstract).

Brodie, J., and White, N. 1994. Sedimentary basin inversion caused by igneous underplating: northwest European continental shelf. Geology 22:147–150.

Campbell, I. H., and Griffiths, R. W. 1990. Implications of mantle plume structure for the evolution of flood basalts. Earth Planet. Sci. Lett. 99:79–93.

Chen, Z. L. 1985. Permian carbonate gravity flow sediments in the western margin of Yangtze Craton. Lithofacies and Paleogeog. 2:43–50 (in Chinese with English abstract).

Chung, S.-L., and Jahn, B.-M. 1995. Plume-lithosphere interaction in generation of the Emeishan flood basalts at the Permian-Triassic boundary. Geology 23: 889–892.

Chung, S.-L.; Jahn, B.-M.; Wu, G.; Lo, C.-H.; and Cong, B. 1998. The Emeishan flood basalt in SW China: a mantle plume initiation model and its connection with continental break-up and mass extinction at the Permian-Triassic boundary. *In* Flower, M.; Chung, S.-L.; Lo, C.-H.; and Lee, T.-Y., eds. Mantle dynamics and plate interaction in east Asia. AGU Geodynamics Series 27:47–58.

Cox, K. G. 1989. The role of mantle plumes in the development of continental drainage patterns. Nature 342:873–877.

Crough, S. T. 1983. Hotspot swells. Annu. Rev. Earth Planet. Sci. 11:165–195.

D'Acremont, E.; Leroy, S.; and Burov, E. B. 2003. Numerical modelling of a mantle plume: the plume head-lithosphere interaction in the formation of an oceanic large igneous province. Earth Planet. Sci. Lett. 206: 379–396.

Dam, G.; Larsen, M.; and Sønderholm, M. 1998. Sedimentary response to mantle plumes: implications from Paleocene onshore successions, west and east Greenland. Geology 26:207–210.

ECS (Editing Committee of Stratigraphy). 2000. Permian in China. Beijing, Geological Publishing House, 149 p.

Farnetani, C. G., and Richards, M. A. 1994. Numerical investigation of the mantle plume initiation model for flood basalt events. J. Geophys. Res. 99:13,813–13,833.

Feng, Z. Z.; Yang, Y. Q.; and Jin, Z. K. 1997. Lithofacies paleography of Permian of south China. Beijing, Petroleum University Press, 242 p. (in Chinese with English abstract).

Griffiths, R. W., and Campbell, I. H. 1990. Stirring and structure in mantle plume. Earth Planet. Sci. Lett. 99: 66–78.

———. 1991. Interaction of mantle plume heads with the Earth's surface and onset of small-scale convection. J. Geophys. Res. 96:18,275–18,310.

Hanski, E.; Walker, R. J.; Huhma, H.; Polyakov, G. V.; Balykin, P. A.; Hoa, T. T.; and Phuong, N. T. 2004. Origin of the Permian-Triassic komatiites, northwestern Vietnam. Contrib. Mineral. Petrol. 147:453–469

He, B.; Xu, Y.-G.; Chung, S.-L.; Xiao, L.; and Wang, Y. 2003. Sedimentary evidence for a rapid, kilometer-scale crustal doming prior to the eruption of the Emeishan flood basalts. Earth Planet. Sci. Lett. 213: 391–405.

Huang, K.; Opdyke, N. D.; Peng, X.; and Li, J. 1992. Paleomagnetic results from the upper Permian of the eastern Qiangtang Terrane of Tibet and their tectonic implications. Earth Planet. Sci. Lett. 111:1–10.

Jin, Y. G.; Utting, J.; and Wardlaw, B. R., eds. 1994. Permian stratigraphy, environments and resources. Paleoworld. Vol. 9, pt. 1. Nanjing, Nanjing University Press.

Liang, D. Y.; Nie, Z. T.; and Song, Z. M. 1994. Extensional Dongwu movement in the western margin of Yangtze Craton. Earth Science 7:443–453 (in Chinese with English abstract).

Liang, D. Y.; Nie, Z. T.; Wan, X. Q.; and Chen, G. M. 1991. On the seismite and seismodisconformity: example from W Sichuan and W Yuannan. Geoscience 5:138–146 (in Chinese with English abstract).

Liu, J. H.; Liu F. T.; He, J. K.; Chen, H.; and You, Q. Y. 2001. Study of seismic tomography in Panxi paleorift area of southwestern China: structural features of crust and mantle and their evolution. Sci. China D 44:277–288.

Luo, Z.; Jin, Y.; and Zhao, X. 1990. The Emei taphrogenesis of the upper Yangtze platform in south China. Geol. Mag. 127:393–405.

MacLennan, J., and Lovell, B. 2002. Control of regional sea level by surface uplift and subsidence caused by

This content downloaded from 23.235.32.0 on Sun, 11 Oct 2015 09:15:18 AM
All use subject to JSTOR Terms and Conditions

magmatic underplating of Earth's crust. Geology 30: 675–678.

McKenzie, D. 1984. A possible mechanism for epeirogenic uplift. Nature 307:616–618.

Mullins, D., and Neumann, A. 1979. Deep carbonate bank margin structure and sedimentation in the northern Bahamas. *In* Doyle, L. J., and Pilkey, O. H., eds. Geology of continental slopes. SEPM Spec. Publ. 27:165–192.

Nadin, P. A.; Kusznir, N. J.; and Cheadle, M. J. 1997. Early Tertiary plume uplift of the North Sea and Faeroe-Shetland basins. Earth Planet. Sci. Lett. 148:109–127.

Rainbird, R. H. 1993. The sedimentary record of mantle plume uplift preceding eruption of the Neoproterozoic Natkusiak flood basalt. J. Geol. 101:305–318.

Rainbird, R. H., and Ernst, R. E. 2001. The sedimentary record of mantle-plume uplift. *In* Ernst, R. E., and Buchan, K. L., eds. Mantle plumes: their identification through time. Geol. Soc. Am. Spec. Publ. 352:227–245.

Thomas, D. N.; Rolph, T. C.; Shaw, J.; Gonzalez de Sherwood, S; and Zhuang, Z. 1998. Paleointensity studies of a Late Permian lava succession in Guizhou Province, south China: implications for post-Kiaman dipole field behaviour. Geophys. J. Int. 134:856–866.

Wang, L. T.; Lu, Y. B.; Zhao, S. J.; and Luo, J. H. 1994. Permian lithofacies paleogeography and mineralization in south China. Beijing, Geological Publishing House, 147 p. (in Chinese with English abstract).

White, N., and Lovell, B. 1997. Measuring the pulse of a plume with the sedimentary record. Nature 387:888–891.

White, R. S.; Spence, G. D.; Fowler, S. R.; McKenzie, D. P.; Westbrook, G. K.; and Bowen, A. N. 1987. Magmatism at rifted continental margins. Nature 330: 439–444.

Williams, G. E., and Gostin, V. A. 2000. Mantle plume uplift in the sedimentary record: origin of kilometer-deep canyons within late Neoproterozoic successions, South Australia. J. Geol. Soc. Lond. 157:759–768.

Xiao, L.; Xu, Y.-G.; Chung, S.-L.; He, B.; and Mei, H. J. 2003. Chemostratigraphic correlation of upper Permian lava succession from Yunnan Province, China: extent of the Emeishan large igneous province. Int. Geol. Rev. 45:753–766.

Xu, Y.; Chung, S.-L.; Jahn, B.-M.; and Wu, G. 2001. Petrologic and geochemical constraints on the petrogenesis of Permian-Triassic Emeishan flood basalts in southwestern China. Lithos 58:145–168.

Xu, Y.-G.; He, B.; Chung, S.-L.; Menzies, M. A.; and Frey, F. A. 2004. Geologic, geochemical, and geophysical consequences of plume involvement in the Emeishan flood-basalt province. Geology 32:917–920.

Xu, Y.-G.; Mei, H. J.; Xu, J. F.; Huang, X. L.; Wang, Y. J.; and Chung, S.-L. 2003. Origins of two differentiation trends in the Emeishan flood basalts. Chin. Sci. Bull. 48:390–394.

Yang, Z. Y. 1986. The Permian system. *In* Yang, Z. Y.; Cheng, Y. Q.; and Wang, H. Z., eds. The geology of China. Oxford, Clarendon, 303 p.

Zhang, Y. X.; Luo, Y. N.; and Yang, Z. X. 1988. Panxi rift. Beijing, Geological Publishing House, 466 p. (in Chinese with English abstract).

Zhang, Z. C., and Wang, F. S. 2002. Permian picritic lava discovered in the Emeishan large igneous province. Geol. Rev. 48:448–448 (in Chinese with English abstract).

Zhao, X. K. 1991. Analysis of late Middle Permian Zhijin basin prototype in central Guizhou. Oil Gas Geol. 12: 308–322 (in Chinese with English abstract).

This content downloaded from 23.235.32.0 on Sun, 11 Oct 2015 09:15:18 AM
All use subject to JSTOR Terms and Conditions